Infant Retinal Images Optic Disk Detection Using Active Contours

Thammanoon Charmjuree*, Bunyarit Uyyanonvara**, Stanislav S. Makhanov***
School of Information & Technology Management, Sirindhorn International Institute of Technology , Thammasart University, Bangkok, Thailand
*(Tel : +66-1-629-5624; E-mail: thammanoonc@siit.tu.ac.th)
**(Tel : +66-2-501-3505; E-mail: bunyarit@siit.tu.ac.th)
***(Tel : +66-2-501-3505; E-mail: makhanov@siit.tu.ac.th)

Abstract: The paper presents a technique to identify the boundary of the optic disc in infant retinal digital images using an approach based on active contours (snakes). The technique can be used to be develop a automate system in order to help the ophthalmologist's diagnosis the retinopathy of prematurity (ROP) disease which may occurred on preterm infant,. The optic disc detection is one of the fundamental step which could help to create an automate diagnose system for the doctors we use a new kind of active contour (snake) method has been developed by Chenyang et. al. [1], based on a new type of external force field, called gradient vector flow, or GVF. GVF is computed as a diffusion of the gradient vectors of a gray-level or binary edge map derived from the image. The testing results on a set of infant retinal ROP images verify the effectiveness of the proposed methods. We show that GVF has a large capture range and it's able to move snakes into boundary concavities of optic disc and finally the optic disk boundary was determined.

Keywords: Retinopathy of Prematurity, Optic Disk Detection, Active Contour, Infant Retinal Image

1. INTRODUCTION

The current method to recognize the ROP disease is to see from the infant retinal image which normally acquired from the new generation of retinal imaging cameras, RetCam 120^{TM} shown in the Figure 1, allows documentation of nearly the entire retina with immediate and permanent image storage of 640x480 pixels of 24 bit RGB bitmaps. The disadvantage of this system is the variable image quality arising during the examination of the eye caused by factors such as movement by the infant, the imperfect geometry of the undeveloped eye and the size of the retina (~14mm c.f.21-23mm adult). The system is shown in the Figure 2.

Fig 1. The RetCam 120TM system

Fig 2. An infant Undergoing screening for ROP

The development of automatic infant retinal image analyzing and diagnosing system has been the ultimate objective of our work to facilitate clinical diagnosis. Localization or extraction of the normal and abnormal features in infant retinal images is a fundamental step to be further developed into the fully functional system in the future. The normal features of retinal images include optic disc, fovea and blood vessels. The growths of abnormal blood vessels in the retina are the main features for prematurity retinopathy, which is the leading cause of blindness in the infants. The retinopathy of prematurity is a disease of the eyes of prematurely born infants in which the retinal blood vessels increase in number and branch excessively, sometimes leading to hemorrhage or scarring [2].

Retinopathy of prematurity (ROP) will be severely threatening to premature infant's eye sight if the condition could not be detected and the appropriate treatment could not be given in the right time. The detection of infant retinal optic disk is the starting point to develop image processing technique which it's used to facilitate the ROP detection.

The ROP is also known as Retrolental Fibroplasia, generally begins during the first few days of life and may process rapidly to blindness over a period of weeks. This happens because the eye is rapidly developing during 28-40 weeks gestational. The blood supply to the retina starts at the optic nerve at about 16 weeks and blood vessels grow out from there toward the edges of the retina until the time of birth. When a baby is born prematurely, this normal vessel growth stops and new abnormal vessels begin to grow. Over time this vessel growth produces a fibrous scar tissue which attaches to the retina and the vitreous gel that gives the eyeball its shape. This ring may extend 360 degrees around the inside of the eye. If enough scar tissue forms, it can begin to pull the retina, detaching it, and, in some cases, causing blindness [3]. Many researchers tried to evaluate ROP by comparing it with reference images which shown in Figure 3.

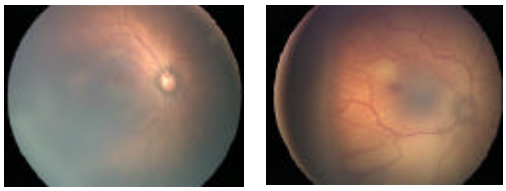

Fig 3, (left) represents normal vessels and (right) show infant retinal image with ROP

The optic disc is the exit point of retinal nerve fibers from

the eye, and the entrance and exit point for retinal blood vessels. It is a brighter region than the rest of the ocular fundus and its shape is approximately round. The location of the optic disc is crucial in retinal image analysis, for example, as a reference to measure the distances and identify anatomical parts in retinal images (e.g. the fovea), for blood vessel tracking, and many others [4].

The methodology of how to detect the boundary of optic disc was developed mainly concentrated working on the general adult fundus images and locating its centre only [5,6,7]. For example, Sinthanayothin et al. [6] used an 80x80 sub-image to evaluate the intensity variance of adjacent pixels, marking the point with the largest variance as the optic disc center. Lalonde et al. [7] localized the optic disc using Hausdorff-based template matching and pyramidal decomposition. They reported an average error of 7.0% in locating the disc centre and 80% area overlap between their groundtruth optic disc and their localized one. Most reported works do not address accurate optic disc boundary identification and also on adult fundus image only and a few of them did experiments on infant images. In this paper, we build on an existing GVF snake method reported by Chenyang et al. [1] with ROP fundus images in order to determine an accurate localization of the optic disc.

2. ACTIVE CONTOUR MODEL (OR SNAKE)

In this section, we review the mathematic formulation of conventional snakes and GVF snakes. We also describe the strengths and weakness of each method.

2.1 Traditional Snake

The snake or active contour model was originally proposed by Kass et at. [9] to solve the problem of how to represent a set of points which have been determined to lie on an edge, which has the advantage that the final form of a contour can be influenced by feedback from a higher level process. A snake is a curve that moves towards the sought for shape in a way that is controlled by internal forces such as rigidity, elasticity, and an external image force. The images should attract the contour to certain features, such as edges, in the image this done by creating an attractor image, which defines how strongly each point in the image should attract the contour. After the contour has been well defined on one slice of a volume data by a 2D-segmentation method, the contours of the subsequent slices can be obtained through the modified snake method. These active contours are examples of the general technique of matching deformable models to image data by means of energy minimization [10,11]. Snakes are represented parametrically, with each position denoted as v(s) = (x(s), y(s)) and the snake being controlled by an energy functional E_{snake} which it is associated with the contour, and consists of terms dependent on internal and external influences:

$$E_{snake} = \int_0^1 \left[E_{\text{int}}(v(s,t)) + E_{ext}(v(s,t)) \right] ds \quad \text{.....(1)}$$

where $E_{\text{int}}(v)$ represents the internal energy of the contour due to kinetic and potential energy terms, and $E_{ext}(v)$ represents energy due to an external energy field generated by the image in which the contour is embedded. The internal energy term can be represented as follows [9,12]:

$$E_{\text{int}}(v) = \frac{1}{2}\left[\mu \left| \frac{\partial^2 v}{\partial t^2} \right|^2 + \alpha \left| \frac{\partial v}{\partial s} \right|^2 + \beta \left| \frac{\partial^2 v}{\partial s^2} \right|^2 \right] \quad \text{.....(2)}$$

where α quantifies the elasticity of the contour (resistance to stretching), and β determines the rigidity of the snake (resistance to bending). More general formulations are possible in which μ, α and β are themselves parameterized by s, but in this paper we assume global fixed values for these coefficients. The first term in Eq. (2) is a kinetic energy term, related to the differential motion of the contour at each point. The second term characterises the potential energy due to stretching of the contour, and is a generalisation of Hooke's law, in which potential energy is proportional to squared extension. The third term represents the potential energy due to bending. In many cases, the mass density of the snake is assumed to be zero so that only the last two terms of Eq. (2) are shown. The external energy E_{ext} represents the effect of forces that are not intrinsic properties of the contour, but which are image dependent. Commonly used definitions of external energy fields include [18]:

$$E_{ext}(x,y) = \begin{cases} E_{ext}^{(1)}(x,y) = -\left|\nabla I(x,y)\right|^2 \\ E_{ext}^{(2)}(x,y) = -\left|\nabla \left[G_\sigma * I(x,y) \right]\right|^2 \end{cases} \quad \text{.(3)}$$

where ∇ is the gradient operator, $*$ is the convolution operator, and G_σ is a 2D symmetric zero-mean Gaussian function parameterized by σ. The first of these external energy fields has minima at place of high image gr adient, *e.g.,* edges. The second formulation has minima at location where a Gaussian filtered image has maxima, and provides a more diffuse external field. Note that both of these external energy fields are conservative (irrotational), i.e., $\nabla \times \nabla E = 0$.

Although the traditional snakes have found and used for such a long time in many applications, but they still have some of the disadvantages or some of the problems still persists i.e. Suhuai *et at.* [8] claimed that they have intrinsically weak in three main aspects: Fist, they are very sensitive to parameters. Second they have small capture range and the convergence of the algorithm is mostly dependent of the initial position. Finally, they have difficulties in processing into boundary concavities. Chenyang *et. al.* [1] found that first, the initial contour must, in general, be close to the true boundary or else active contour will likely converge to the wrong result which several methods have been proposed to address this problem including multiresolution methods[14], pressure forces [13] and distance potentials[15] to increase the capture range of the external force fields and to guide to the contour toward the desired boundary. The second problem is that active contours have difficulties progressing into boundary concavities [16,17] which there is no satisfactory solution to this problem.

2.2 Gradient Vector Flow

From the traditional snakes, we can summarize that there are two general problems with traditional snakes. First, the contour must be initialized closed to the boundary of interest, otherwise there is a high chance the curve will stabilize in a different local minima. Second, classical active contours cannot progress into boundary concavities. To address this problem Chenyang et al. [1] define the GVF, dense nonconservative vector field derived from an image by minimizing a certain energy functional in variational framework to be the vector field $v(x,y)=(u(x,y),v(x,y))$. The basic idea of GVF is to extend influence range of image force to a larger area by generating a GVF field which is computed from the image. Their used solution is a static external force field termed the GVF field $F_{ext}^{GVF}=h(x,y)$:

$$F_{ext}^{GVF}=h(x,y)=\begin{pmatrix}p(x,y)\\ q(x,y)\end{pmatrix} \quad \text{.....(4)}$$

The GVF field $h(x,y)$ is defined to minimize the following energy functional

$$E_{GVF}=\iint_{x\ y}\left[\lambda\left(\left|\frac{\partial p}{\partial x}\right|^2+\left|\frac{\partial p}{\partial y}\right|^2+\left|\frac{\partial q}{\partial x}\right|^2+\left|\frac{\partial q}{\partial y}\right|^2\right)+|\nabla g|^2|h-\nabla g|^2\right]dxdy$$

.....(5)

where g is an edge map of the image I ,*i.e.* $g(x,y)=|\nabla[G_\sigma(x,y)*I(x,y)]|$ and λ is a regularization parameter, which governs the trade-off between the first and second terms in the integrand. The intention is to obtain an extended directional smooth field of attraction, that accounts for the proximity of boundaries, and hence reduces the sensitivity to initializ ation. Qualitatively, this formulation is equivalent to the solution of a generalized diffusion equation, and has the effect of increasing the effective range of edges at locations distant from edges. Conversely, near edges, where $|\nabla g|$ is large, the second term is dominant and can be regulated by setting $h\approx\nabla g$ so that the local accuracy is preserved, Again using the calculus of variation, the GVF field can be found by solving the following Euler equations:

$$\begin{cases}\lambda\nabla^2 p-(p-q_x)(g_x^2+g_y^2)=0\\ \lambda\nabla^2 q-(q-g_y)(g_x^2+g_y^2)=0\end{cases} \quad \text{.....(6)}$$

A numerical solution to Eq. (6) can be found by treating p and q as functions of time, and hence converging to a solution. The iterative solution so obtained is fully in [1], and convergence of this iterative algorithm is guaranteed for certain values of λ .

3. PROPOSED METHOD

The Active Contour s system was deployed in this experiment were developed by Dejan Tomazevic (University of Ljubljana), Chenyang Xu and Jerry L. Prince (Johns Hopkins University) in 1998, using MATLAB development tools. We have tested the GVF snake on many characteristics of object; ultimate experiment goal is to use a GVF snake to find the boundary of ROP infant optic disc. By fitting a GVF snake onto the gray-level ROP images and comparing the resulting region against the traditional snake method, we found that some improvement of the results can be identified which shown in the Figure 4, 5, and 6 Several different gray-level ROP images were tested for the regularization parameters of the GVF, a=0.05 and β=0 to control the snake's tension and rigidity respectively, more details shown in the Table 1. The number of iterations for convergence was determined empirically and set to 500 for all cases.

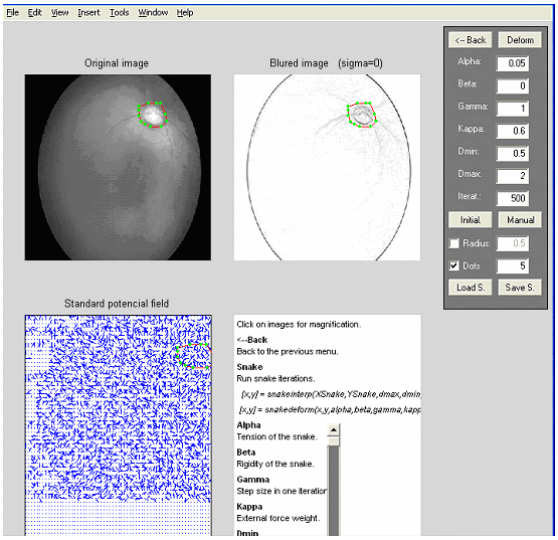

Fig4. Hand labeled initialization

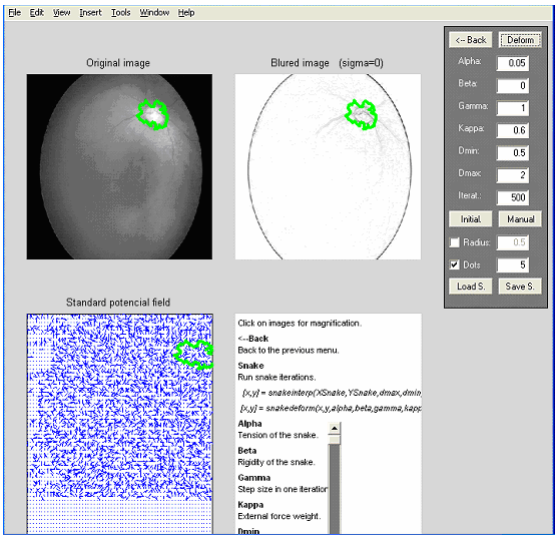

Fig 5. traditional snake results

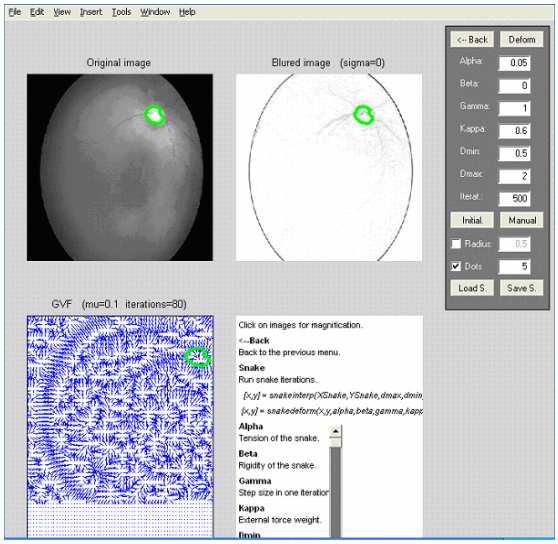

Fig 6. GFV snake results

4. RESULTS

After we applied the Active Contour to images, found that a GVF snake was automatically positioned to detect the boundary of the optic disc in each case and some of the images still face a severeof erroneously to detect an optic disk. We compare the accuracy of the boundary localization against the traditional snake as can be seen in the Figure 7(b), 7(c),8(b) and Figure 8(c).

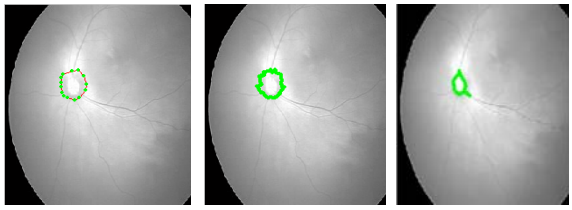

(a) (b) (c)

Fig. 7 Optic Disc boundary detection results; (a) original image with hand labeled initialization; (b) acceptable traditional snake; (c) acceptable GVF snake

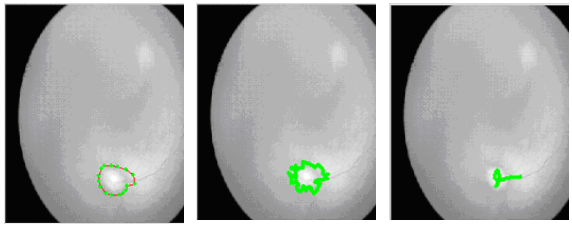

(a) (b) (c)

Fig. 8 Optic Disc boundary detection results; (a) original image with hand labeled initialization; (b) acceptable traditional snake; (c) un-acceptable GVF snake

Alpha	Beta	Gamma	Kappa	Iteration
0.05	0	1	0.6	500

Table 1. The testing parameters

Image No.	Distance from Optic Disc boundary		Remark
	Traditional snake	GVF snake	
1.	Not acceptable	Acceptable	
2.	Not acceptable	Acceptable	
3.	Not acceptable	Acceptable	
4.	Not acceptable	Acceptable	
5.	Not acceptable	Not acceptable	
6.	Not acceptable	Acceptable	
7.	Not acceptable	Acceptable	
8.	Not acceptable	Not acceptable	
9.	Not acceptable	Not acceptable	
10.	Not acceptable	Not acceptable	

Table 2. Comparision Optic Disc boundary detection between traditional snake and GVF snake results

5. CONCLUSION

The results indicate that a GVF-based snake can be used to extract an accurate boundary for the infant optic disk region. We have shown that it allows for flexible initialization of the snake or deformable surface and encourages convergence to boundary concavities. But there are the sensitivity of GVF field technique to ROP image variations was considers two potential sources of variation and the erroneous results may occurred because the GVF field is based on an edge map calculated from the raw image. In some images, the optic disc boundary is not well defined, due to natural variation or pathological changes and/or photographic conditions, e.g. too little or too much light, poor images contrast, etc.

The infant retinal images optic disc detection results may inaccurate for some of the image which depends on the morphology of each image. We found that the original snake does not suitable for infant retinal images as shown in the table 2. To obtain correct convergence onto the boundary of the optic disk, we need to improved the algorithm or its may required some pre-process the image to remove pixels corresponding to vascular structures, and replace them by pixels representative of the optic disk background behind in order to apply with a specific characterization of the images.

REFERENCES

[1] C. Xu, J. Prince, “Snakes, Shapes and Gradient Vector Flow”, IEEE Transaction on IP, 7, No. 3, pp 359-369, 1998.

[2] Donald F. Everett, M.A. National Eye Institue, National Institutes of Health. Cryotherapy for Retinopathy of Prematurity (CRYO-ROP)-Outcome Study of Cryotherapy for Retinopathy of Prematurity.

[3] Kate Moss “Retinopathy of Prematurity”, Family Support Specialist, TSBVI Deafblind Outreach

[4] Alireza Osareh, Majid Mirmehdi, Barry Thomas, and

Richard Markham,"Colour Morphology and Snakes for Optic Disc Localisation", In A Houston and R Zwiggelaar, editors, The 6th Medical Image Understanding and Analysis Conference, pages 21--24. BMVA Press, July 2002.

[5] Li, O. Chutatape, "Automatic Location of Optic Disk in Retinal images", IEEE ICIP, pp. 837-840, 2001.

[6] C. Sinthanayothin, J. Boyce, C.T. Williamson, "Automated Localisation of the Optic Disk, Fovea, and Retinal Blood Vessels from Digital Colour Fundus Images", British Journal of Ophthalmology, 38, pp 902-910, 1999.

[7] M Lalonde, M Beaulieu L Gagnon, "Fast and Robust Optic Disk Detection using Pyramidal Decomposition and Hausdorff- Based Template Matching" IEEE Transaction On Medical Imaging, 20, No. 11, pp 1193-1200, 2001.

[8] Sonka, M., Hlavac, V.,. Boyle, R.: Image Processing, Analysis and Machine

[9] M. Kass, A. Witkin & D. Terzopoulos, "Snakes: Active Contour Models," Proceedings of First International Conference on Computer Vision, 1987, pp. 259-269

[10] M. Kass, A. Witkin, and D. Terzopoulos "Snakes: Active contour models," int. J. Comput. Vis., vol. 1, Jan. 1988, pp. 321-332

[11] D. Terzopoulos, A. Witkin, and M. Kass "Constraints on deformable models:Recovering 3D shape and non rigid motions," Artificial Intelligence, 1988.

[12] Sonka, M., Hlavac, V.,. Boyle, R.: Image Processing Analysis and Machine L. D. Cohen. On active contour models and balloons. CVGIP: Image Understanding, 53(2):211-218

[13] B. Leroy, I. Herlin, and L. D. Cohen,. Multi-resulution algirthms for active contour models. In 12th International Conference on Analysis and Optimization of Systems ,pages 58-65, 1996

[14] L. D. Cohen and I. Cohen. Finite-element methods for active contour models and balloons for 2-D and 3-D images. IEEE Trans. On Pattern Anal. Machine Intell., 15(11):1131-1147, November 1993.

[15] C. Davatzikos and J. L. Prince. An active contour model for mapping the cortex. IEEE Trans. On Medical Imaging, 14(1):65-80, March 1995.

[16] A. J. Abrantes and J. S. Marques. A class of constrained clustering algorithms for object boundary extraction. IEEE Trans., on Image Processing, 5(11):1507-1521, November 1996

[17] Francois Mendels, Conor Heneghan and Jean-Philippe Thiran "Identification of the Optic Disk Boundary in Retinal Images using Active Contours". Signal Processing Laboratory (LTS), Swiss Federal Institute of Technology.